JOURNAL OF AGRICULTURAL AND FOOD CHEMISTRY

Spectroscopic and Thermal Investigations on Compost Improved by Iron Salt Addition

MARIA ROSARIA PROVENZANO,*,† ANTONIO ALBUZIO,§ AND VALERIA D'ORAZIO†

Dipartimento di Biologia e Chimica Agroforestale e Ambientale, Via G. Amendola 165/A, I-70126, Bari, Italy, and Dipartimento di Biotecnologie Agrarie, Strada Romea 16, I-35020 Legnaro, Padova, Italy

A quality compost obtained from sewage sludge (one part in weight) and yard trimmings and sawdust (two parts) has been investigated as a potential carrier of iron to plants. At the end of the thermophilic phase, the composting materials were added with crystalline $FeSO_4 \cdot 7H_2O$ (97%). Chemical properties, respiratory indices, and seed germination tests proved the compost to be suitable as an iron carrier in agriculture. Fourier transform infrared spectroscopy (FT-IR) and fluorescence spectroscopy provided evidence of the effective linking of the iron ion to the organic molecule functional groups, thus preventing the loss of iron ion by leaching and precipitation phenomena and allowing the metal ion to be available to plants as both mineral and organic species. The thermogram obtained on compost without iron was similar to that previously obtained for composted materials of different origins, whereas samples with added iron ion exhibited in addition an exotherm in the medium-temperature region. FT-IR spectra carried out on samples heated at different temperatures indicated a loss of iron ion linked to carboxyl groups.

KEYWORDS: Waste recycling; iron-enriched compost; phytocompatibility; spectroscopic and thermal characterization

INTRODUCTION

In well-aerated soils with neutral pH, the concentration of iron ions in the soil solution ($<10^{-10}$ M) is frequently inadequate for the best growth of most plants ($\sim 10^{-8}$ M). To alleviate iron deficiencies, plants tend to develop two major "strategies": releasing root exudates and modifying their rhizosphere conditions (*1*). The addition of organic matter to soils has been known to increase the water-soluble iron in the soil solution and therefore to enhance the uptake by plant roots. The effectiveness of organo−iron complexes is usually attributed to their similarity to soil organic and humic matter in their capacities for binding and releasing metal ions (*2*). Because soluble soil iron exists mainly as organo−iron complexes, efforts have turned to the use of organic solid wastes as an iron source for sensitive crops in deficient soils (*3*).

Fourier transform infrared spectroscopy (FT-IR) and fluorescence spectroscopy have been applied to the study of humic and fulvic acids and to the characterization of composted materials of different origins and compositions (*4*). More recently, three-dimensional (3D) fluorescence spectra, in which repeated emission scans are collected at numerous excitation wavelengths resulting in excitation−emission matrices (EEMs), have provided detailed information useful to identify fluorescent compounds present in complex mixtures (*5*−*7*). Following interaction with metal ions, organic complexes exhibit changes in the relative intensity of both IR absorption bands and fluorescence peaks that provide evidence of the functional groups involved in metal complexation (*2*, *8*).

Thermal analysis such as differential scanning calorimetry (DSC) can be used to obtain information on the thermal behavior of soil organic matter.

In thermal analysis the sample is subjected to a programmed heating in a controlled atmosphere. The resulting thermogram exhibits endothermic and exothermic peaks occurring at temperatures that are related to the chemical structure and thermal stability of the sample (*9*−*12*).

More recently, DSC analysis has been used as a means to assess compost maturity, providing interesting results when applied to the compost samples without any treatment or extraction performed (*13*−*16*).

Following interactions with metal ions, the organic complexes will show changes in the thermal stability of functional groups involved in metal complexation. As a consequence, they are expected to show different temperatures at which thermal effects occur.

The aim of this paper is to apply chemical analysis, spectroscopic techniques such as FT-IR and fluorescence spectroscopy both as EEM and as synchronous-scan excitation spectra, and thermal analysis in DSC to the characterization of a compost made from sewage sludge and lignocellulosic residues at a 1:2 ratio, fortified with $FeSO_4 \cdot 7H_2O$ salt at two different percentages.

* Corresponding author (telephone +39-080-5442929; fax +39-080-5442850; e-mail Provenza@agr.uniba.it).
† Dipartimento di Biologia e Chimica Agroforestale e Ambientale.
§ Dipartimento di Biotechnologie Agrarie.

10.1021/jf048889g CCC: $30.25
Published on Web 12/30/2004

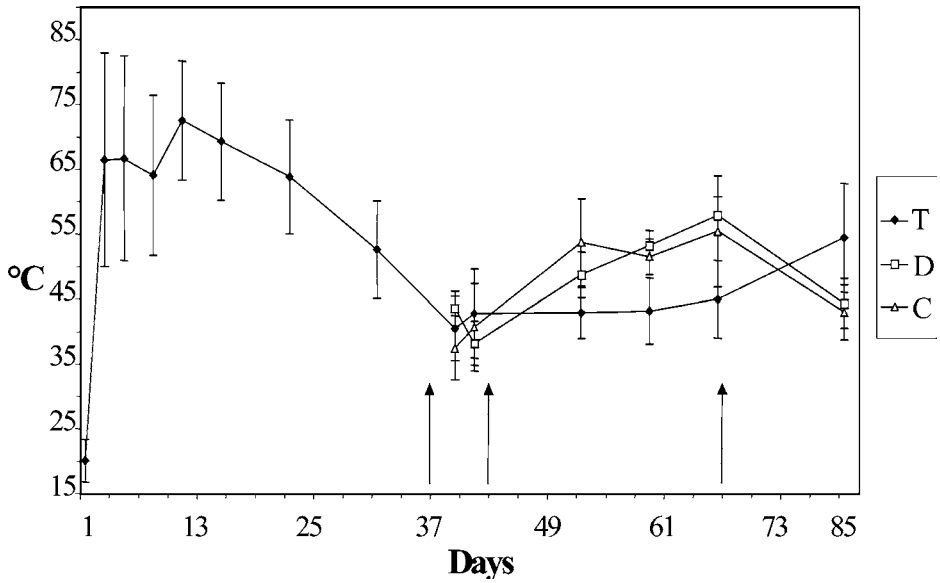

Figure 1. Temperature variation versus biostabilization time. Solid symbols are values for control T. Open symbols are values for 2% (D) and 5% (C) iron-enriched compost. Error bars relate to standard deviation of the mean over five replications. Vertical arrows indicate the mass-turning events.

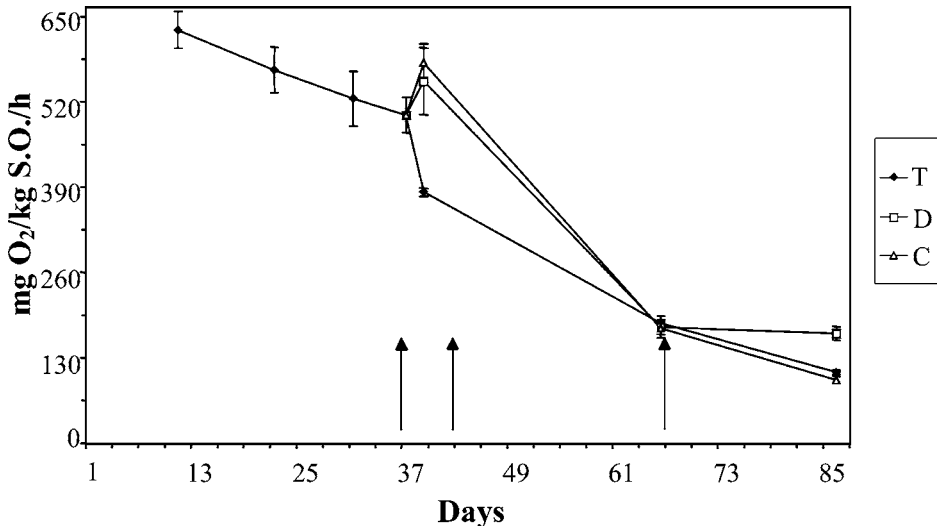

Figure 2. Respiration index variation versus biostabilization time.

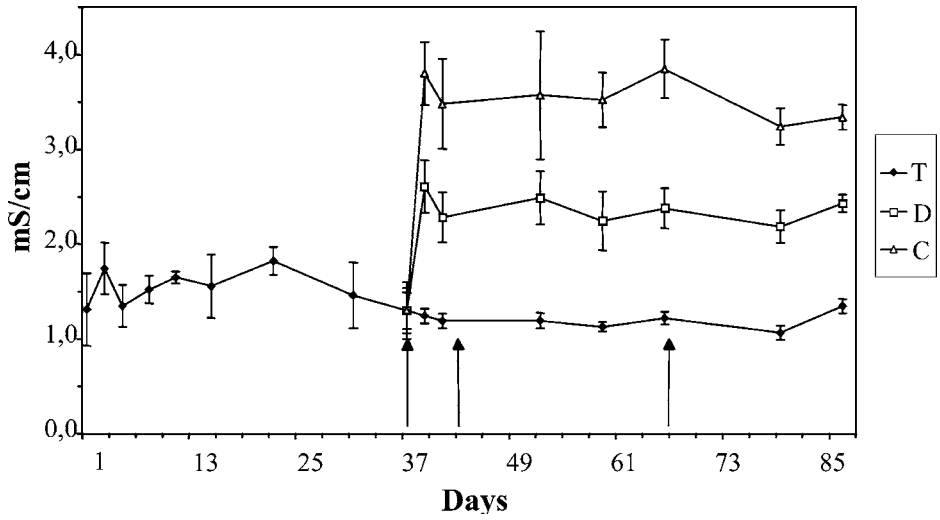

Figure 3. Electrical conductivity versus time.

MATERIALS AND METHODS

The present research has been carried out at a composting facility operated by "Consorzio Tergola" of Vigonza, near Padova, where a quality compost (starting materials selected according to regional standard) is produced by a windrow open system totally enclosed within a building. Alternate forced aeration, controlled by a temperature feed-

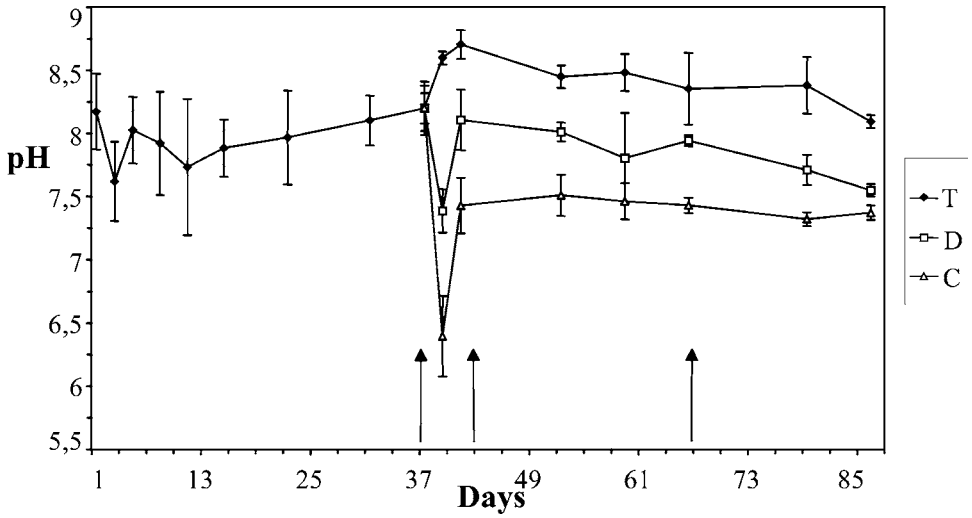

Figure 4. pH variation versus time.

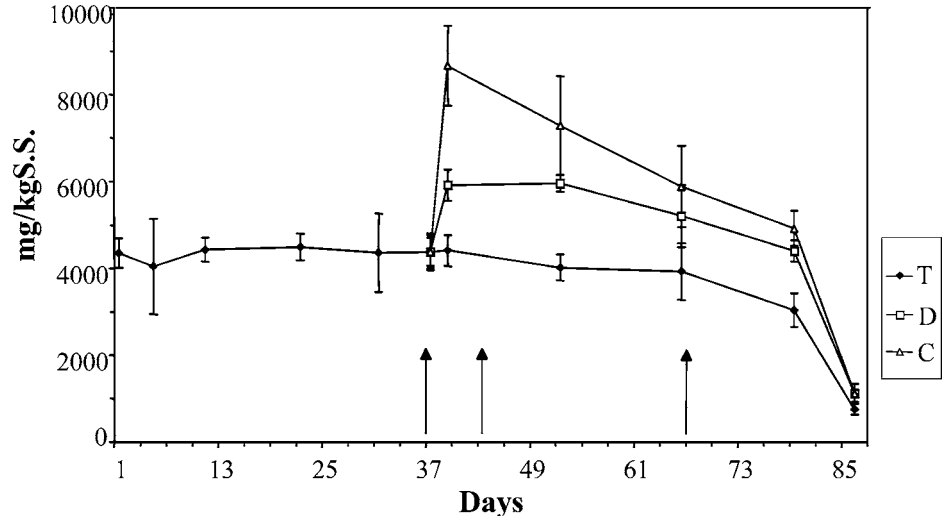

Figure 5. Ammonium N variation versus time.

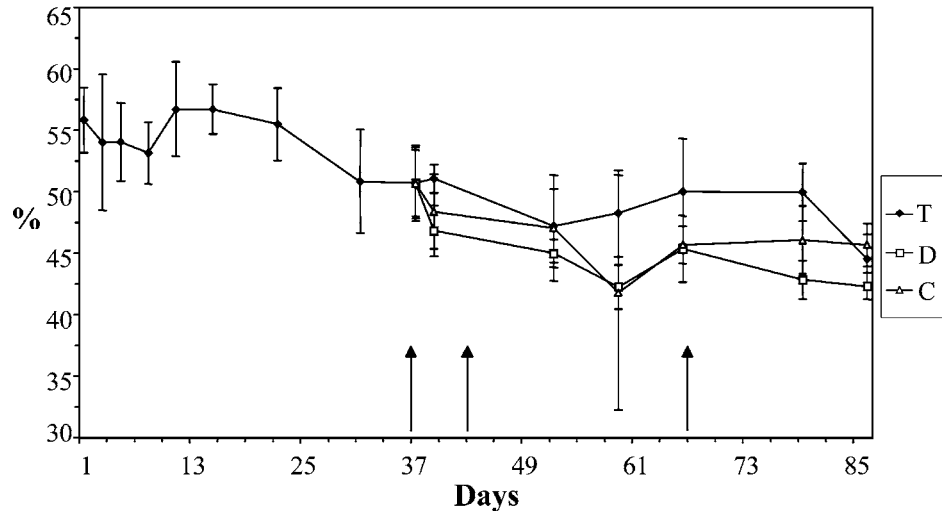

Figure 6. Organic matter content versus time.

back actuation, was operated in conjunction with periodic turning of the piles by a front-end loader. The building was insulated to minimize condensation and was connected to an odor-controlling biofilter with the capacity to deal with the exhaust air from the entire structure. Spray equipment was used to apply water to the composting materials. The percolating solutions were collected by a network of drain pipes.

The composting facility, designed to treat 28000 tons/year of mixed organic residuals, produces good-quality compost, according to speci-

Table 1. Iron Content, Water-Soluble Fraction, and Organo–Iron and Mineral Iron Fractions (Milligrams of Fe per Gram of Compost)[a]

	total Fe	organic Fe	mineral Fe	soluble Fe
T	13.7 f	3.0 e	10.5 ef	0.5 g
D	23.4 c	4.2 c	18.2 c	1.0 e
C	31.4 b	6.4 b	23.3 a	1.6 d

[a] Means in the same column with the same letter(s) are not significantly different at $P \leq 0.05$.

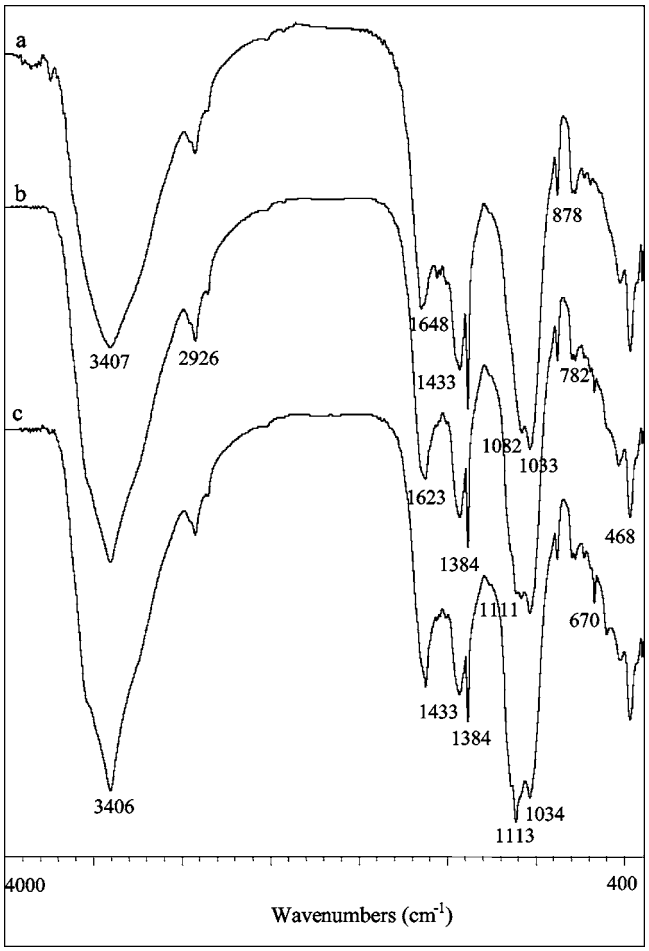

Figure 7. FT-IR spectra of control T sample (**a**), D sample (**b**), and C sample (**c**).

fication no. 766 adopted by the Regione Veneto on September 10, 2000, to be employed on land for crop production and in formulating organic substrates for ornamental plants and in tree nurseries.

Organic Substrate. The organic mixture, to be transformed in the co-composting process, contained one part in weight of municipal sewage sludge (qualitatively in accordance with the criteria required by the above cited legislation) and two parts of shredded lignocellulosic yard trimming and sawdust.

For the iron addition, crystalline $FeSO_4 \cdot 7H_2O$ (97%) was employed.

Composting Procedure. Starting materials were piled in three rows 110 m long, 4 m wide at the base, and 3 m high. An initial phase of suction aeration allowed core temperatures to naturally reach 65−75 °C. The air flow was then reversed, driving it out to the peripheral regions, and thereafter the process proceeded efficiently with alternate forced aeration. Water was added in conjunction with humidity feedback controls operating within 53−58% during the first 30 days and within 42−47% thereafter.

At the end of the thermophilic oxidative phase (36 days from starting), the air flow was stopped and the material was drum-screened through 20 mm square perforations to obtain a suitable particle size and to remove noncompostable items (parent pile). Then, the material

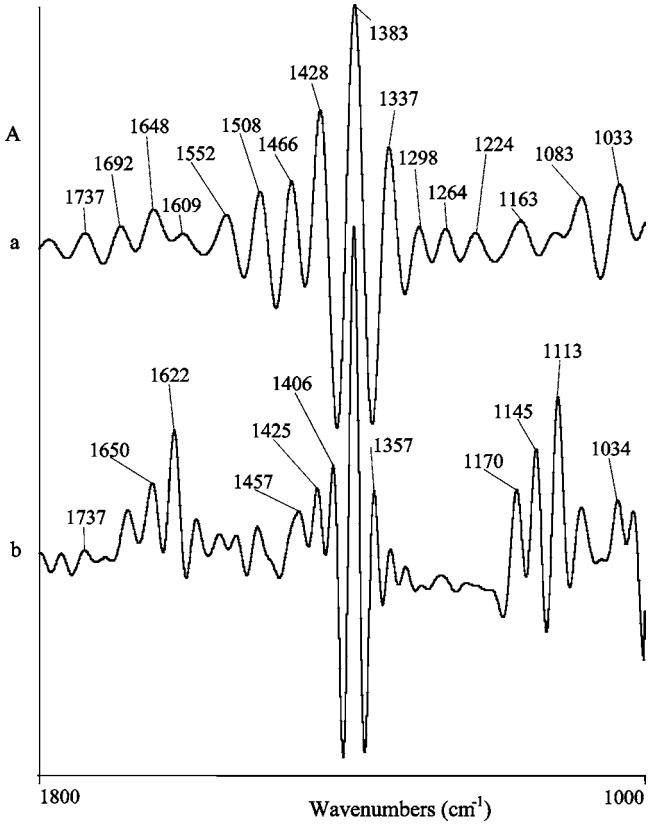

Figure 8. FSD spectra of control T sample (**a**) and C sample (**b**).

was transferred on a concrete base and left to "stabilize" until the 86th day with two turnings (on the 43rd and 67th days).

Addition of Ferrous Sulfate. After the thermophilic oxidative bioconversion (on the 37th day), three experimental piles of small dimensions (14 tons each) were set up with screened materials from the parent pile. Two of them were mixed with ferrous sulfate ($FeSO_4 \cdot 7H_2O$, 97%) in the amounts of 2% (D) and 5% (C) by weight. The third, without iron addition, was considered as a control (T).

Sample Collection. Samples were collected during the thermophilic phase (from the 1st to the 15th day) every 3rd day and after the iron addition (from the 37th to the 41st day). In the other periods of bioconversion, samples were collected every 7th day.

Analytical Methods. The parameters connected to the kinetics of the composting process and to the product quality for agricultural utilization (temperature, humidity, pH, conductibility, total and ammoniac nitrogen, organic carbon, and crop germination index) were determined by applying the methods adopted by Regione Piemonte (*17*).

The evaluation of biological stability evolution (i.e., the decreasing of highly reactive molecules due to microbial activity) was assessed by Static Respiration Index determinations (*18*) and germination indices (*19*).

Total iron concentration was determined by an inductively coupled plasma procedure after sample mineralization (*20*) using a Spectro Ciros ICP-OES 125-769 instrument of Spectro Analytical Instruments Kleve (Germany); the water-soluble iron and the iron bonded with organic substances were determined by water extraction and by an additional extraction with sodium pyrophosphate water solution according to the official Italian methodology (*21*).

All chemicals used were of analysis grade and were purchased from Aldrich (Sigma-Aldrich, Milano, Italy).

FT-IR Spectroscopy. FT-IR spectra were obtained in the 4000 to 400 cm^{-1} wavelength range by a Nicolet 5PC FTIR spectrophotometer on KBr pellets obtained by pressing, under reduced pressure, uniformly prepared mixtures of 1 mg of sample and 400 mg of KBr, spectrometry grade, with precaution taken to avoid moisture uptake.

Fluorescence Spectroscopy. Contour maps of EEM and conventional synchronous scan spectra were obtained on water extracts of whole composts at a concentration of 500 mg L^{-1} after overnight

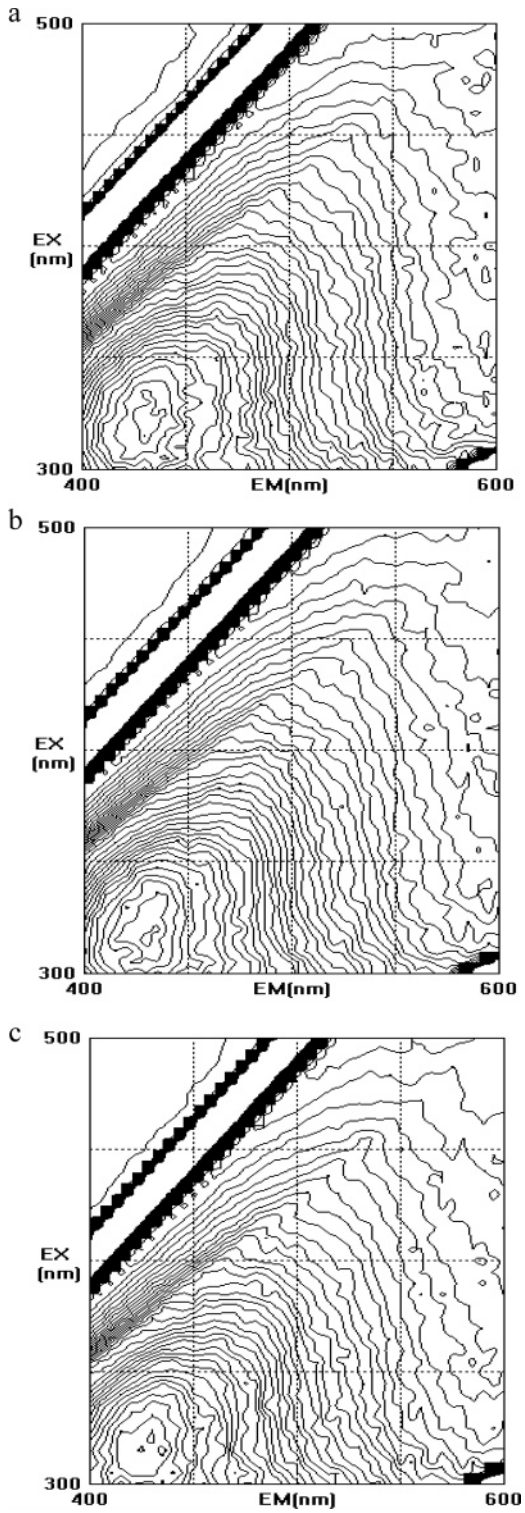

Figure 9. Contour maps of T sample (**a**), D sample (**b**), and C sample (**c**).

equilibration at room temperature (~20 °C) and successive filtration through Whatman no. 2 paper. For comparison with previous data (*21*) the pH was adjusted to 8 with 0.05 N NaOH. A Hitachi model F-4500 fluorescence spectrophotometer was used, equipped with an F-4500 system program for data processing. To obtain EEM maps, the emission (Em) wavelength range was fixed from 400 to 600 nm, whereas the excitation (Ex) wavelength was increased from 300 to 500 nm by 5 nm steps. Synchronous-scan excitation spectra were measured by scanning simultaneously both the excitation, varied from 300 to 550 nm, and emission wavelengths while maintaining a constant, optimized wavelength difference $\Delta\lambda = \lambda_{em} - \lambda_{ex} = 18$ nm.

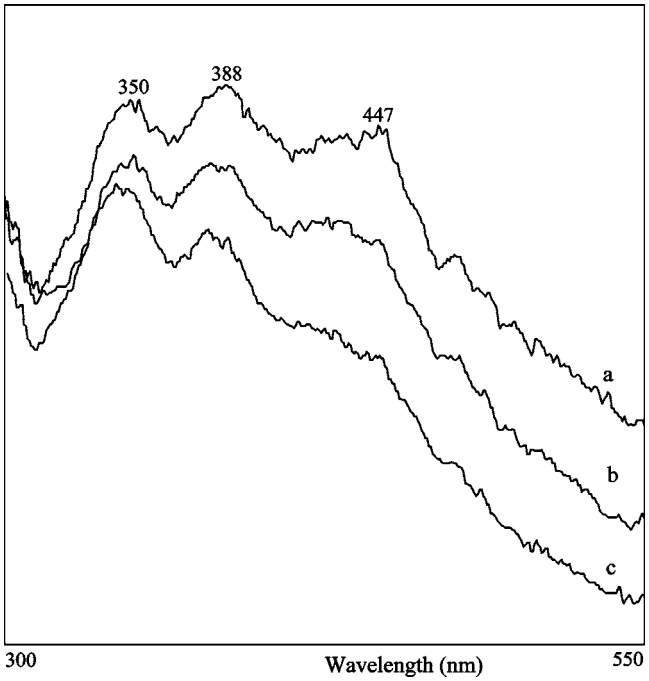

Figure 10. Synchronous-scan excitation spectra of T sample (**a**), D sample (**b**), and C sample (**c**).

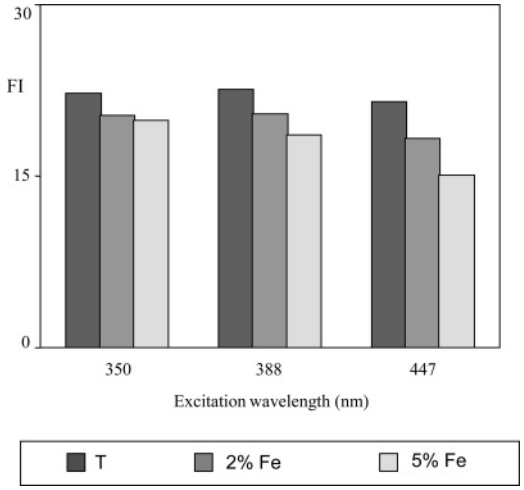

Figure 11. Fluorescence intensity of primary peaks of the three samples.

Differential Scanning Calorimetry. The DSC measurements were performed by a Perkin-Elmer DSC 7 equipped with an automatic program of thermal analysis on intact compost samples without any treatment or extraction performed. Aliquots of 10 mg samples were placed in an aluminum pan of 50 μL capacity and 0.1 mm thickness and press-sealed with a 0.1 mm thick not-pierced aluminum cover. An empty pan sealed in the same way was used as reference. The DSC traces were recorded by heating the sample from 50 to 550 °C at a 20 °C min^{-1} rate under a 20 cm^3 min^{-1} air flow. Indium was used as a standard for temperature calibration. Each sample was run in triplicate.

RESULTS AND DISCUSSION

Temperature and Respiration Index. The temperature variations in the parent pile corresponded to a regular bio-oxidation within the first 36 days. On the 37th day, the addition of ferrous iron sulfate to the D and C piles caused sharp temperature increments within 5 days (**Figure 1**). These temperature increments indicate the start of bio-oxidative reactions again confirmed also by the determinations of the corresponding respiration indices (**Figure 2**).

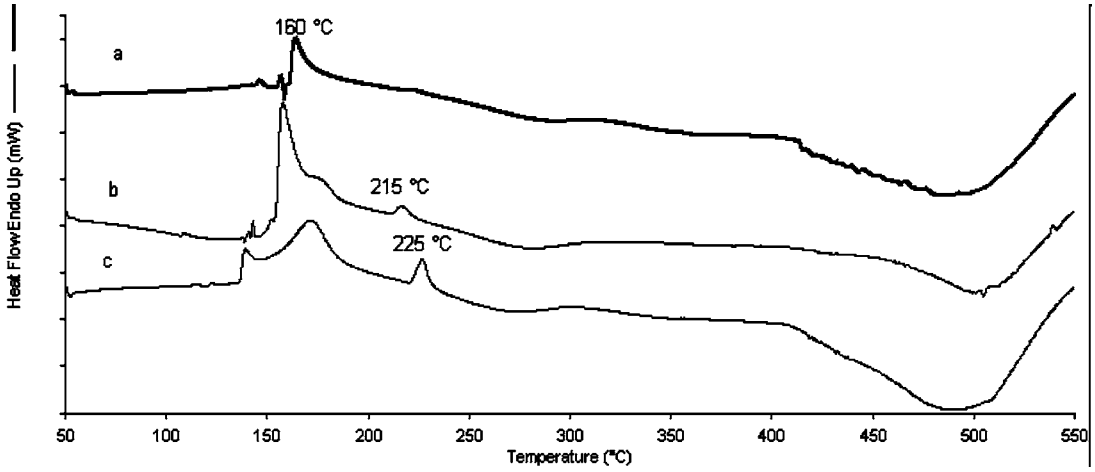

Figure 12. DSC curves of T sample (**a**), D sample (**b**), and C sample (**c**).

Conductivity and Humidity. The conductivity parameters (**Figure 3**) of the parent pile did not change during the thermophilic phase. As expected, the addition of ferrous sulfate to the C and D piles significantly increased conductivity proportional to the amount of mixed iron salt.

During the first 30 days, total humidity was held at an optimum 55% by watering and timed turning of the mass. In the small experimental piles D and C, after the aeration during the screening and after the mass had been turned twice, the humidity decreased to 45% without significant differences among the piles T, D, and C.

pH and Ammonia. The pH values (**Figure 4**) in the parent pile, after small fluctuations during the first 8 days, did not change significantly within 36 days. In experimental pile T, the pH reached 8.5 on the 39th day and then declined to 8.1 on the 86th day. In the D and C piles, the addition of ferrous sulfate caused rapid and large pH decreases to 7.4 and 6.4, respectively. After the 40th day, the materials were neutralized to 7.8 and 7.2, respectively. The acidification is attributed to several concomitant causes: (i) the acidity of the ferrous sulfate as a salt of a weak base with a strong acid; (ii) the absorption of iron ions into the organic substance with the consequent expulsion of protons from ligand groups as carboxylic, phenol, sulfhydrilic, and others; and (iii) the volatilization of ammonia (**Figure 5**) not detectable from the T pile.

Organic Substance and C/N. The content of organic substance (**Figure 6**), influenced by temperature variation and by gaseous emission, decreased from 55 to 45% during the experimental time. The decrease was larger in the piles receiving iron sulfate because of the more intense bio-oxidative processes. The variations of the total nitrogen content (data can be inferred from the C/N rate) started from 19.5%, an unusual content for a composting material due to the high contribution of the municipal sewage sludge; as a consequence, the initial C/N ratio was particularly low (14.5) in comparison with the theoretical values. This situation did not influence either the process evolution or the quality of the final product.

Germination Test. Samples from the T pile, collected on the 36th day, and samples from the D and C piles, collected on the 86th day, were tested for germination index with results >90% in every case. These indicate that the compost, either enriched with iron or unenriched, was phytocompatible.

Distribution of Iron Species. Total iron content [milligrams per gram of dry weight (DW)], the water-soluble fraction, the organo−iron, and the mineral iron fractions are reported in **Table 1**.

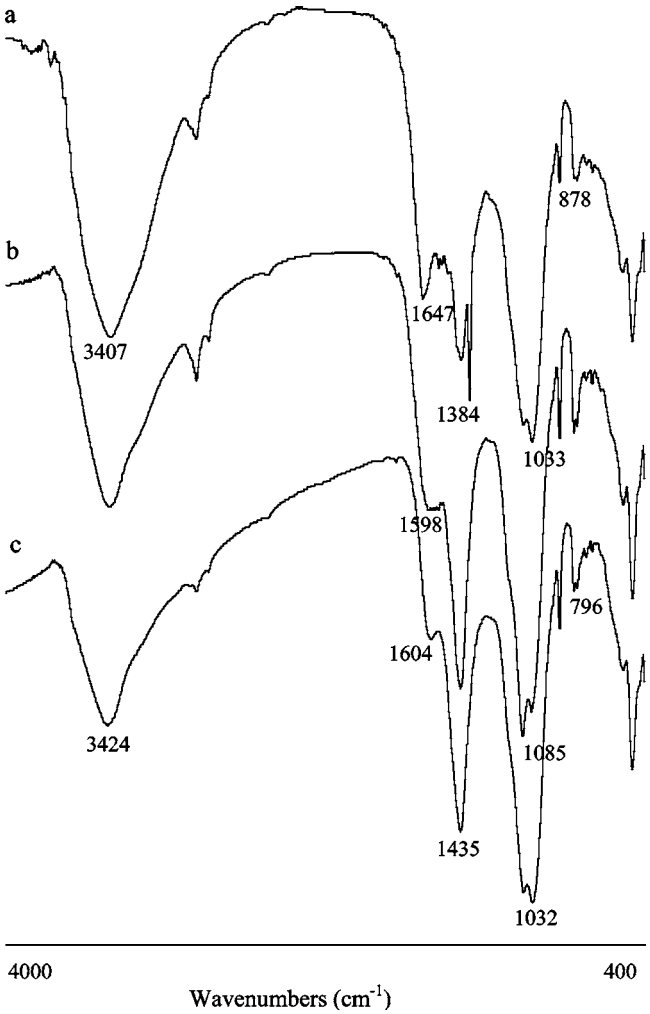

Figure 13. FT-IR spectra of T sample (**a**), T sample heated at 350 °C (**b**), and T sample heated at 550 °C (**c**).

The iron content in the control (T) is in accordance with the data of regular compost, and the iron additions are evidenced in the D and C materials.

Infrared Spectra. The FT-IR spectrum of the T sample (control) is reported in **Figure 7a**. It features the following peaks: about 3400 cm^{-1} (H-bonded OH stretching); about 2925 and 2860 cm^{-1} (aliphatic C−H stretching); about 1648 cm^{-1} (preferentially aromatic C═C vibrations, C═O stretching of amide groups, amide I, possibly originating from incorporated

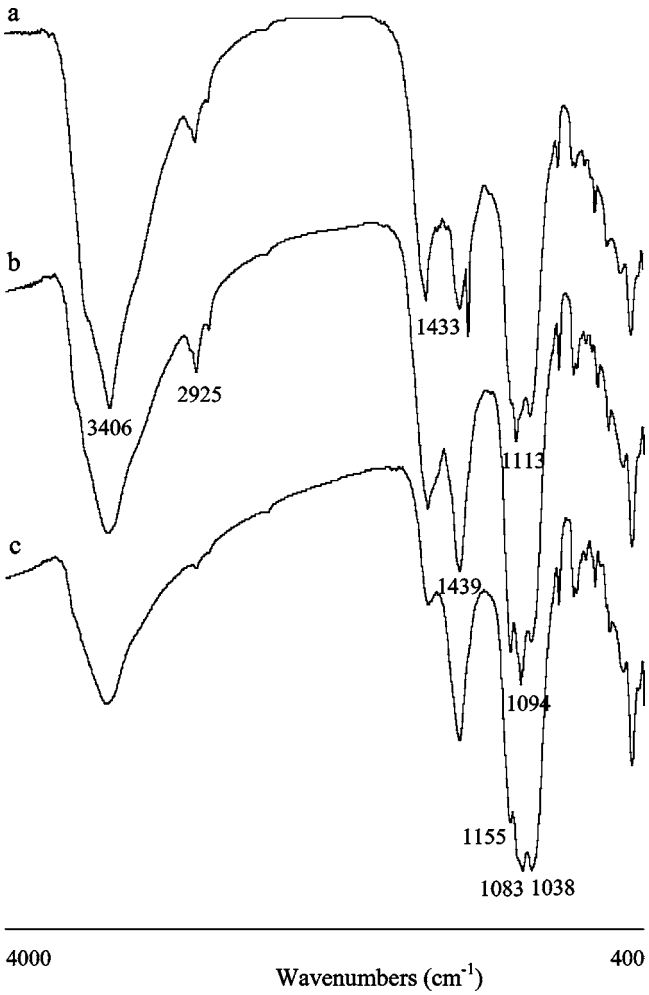

Figure 14. FT-IR spectra of C sample (**a**), C sample heated at 350 °C (**b**), and C sample heated at 550 °C (**c**).

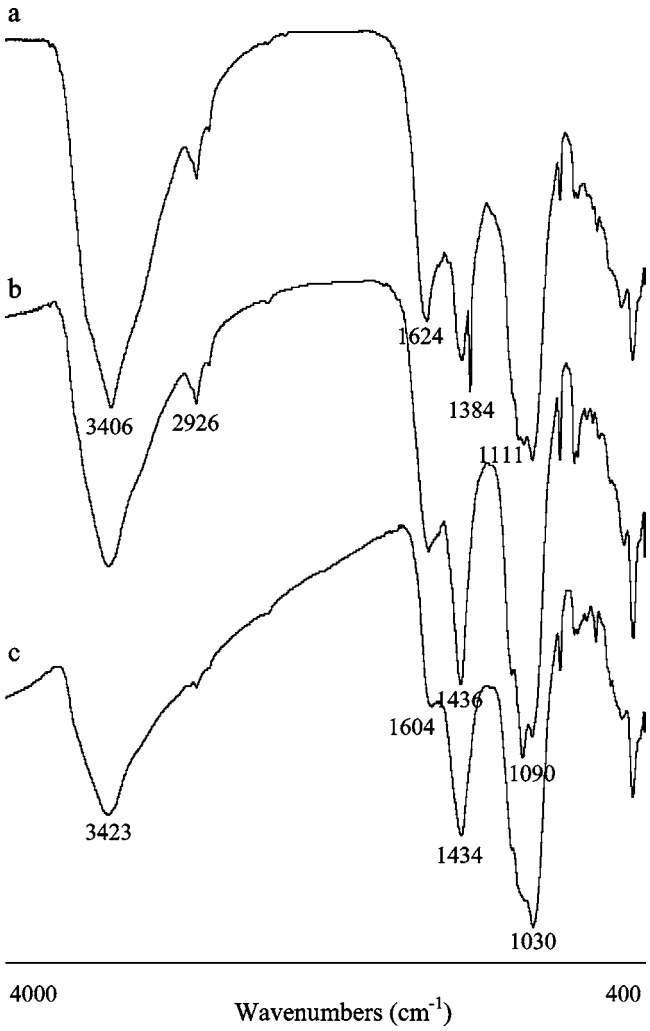

Figure 15. FT-IR spectra of D sample (**a**), D sample heated at 350 °C (**b**), and D sample heated at 550 °C (**c**).

proteinaceous materials in which composts are rich and asymmetric stretching of COO^-); 1506 cm^{-1} (amide II); about 1430 cm^{-1} (aromatic skeletal vibrations of lignin); 1384 cm^{-1} (COO^- groups); 1082 cm^{-1} (various vibrations of graminaceous lignin structures); 1033 cm^{-1} (C−O stretching of polysaccharides, most likely cellulose and residual hemicellulose and other polyols, which are common constituents of sludges).

FT-IR spectra of D (2% Fe) and C (5% Fe) samples (**Figure 7b**,**c**) are similar to the T spectrum, but changes in relative intensities of peaks occur. In particular, 1433 and 1384 cm^{-1} bands become progressively less intense, suggesting that structures responsible for these absorptions are involved in iron interactions. In addition, a small peak appears in D sample at 1111 cm^{-1}, attributed to vibration of hydrated iron ions. This peak appears to be very sharp in C sample, proving the effective linking of this ion to the functional groups of organic molecules.

To better evidence absorption bands, FT-IR spectra were subjected to a Fourier self-deconvolution (FSD) procedure. FSD is a special fast Fourier transform (FFT) filter that synthetically narrows the effective trace bandwidth features. The FFT is the basis for computer-based spectrum analysis, which relies on the representation of a signal in the frequency domain and is one of the most commonly used methods to analyze signals and waveforms. Thus, this analysis seems to be a powerful tool to identify the principal bands that make up a more complex band with overlapping features.

In **Figure 8** deconvoluted spectra of T and C samples in the region 1800−1000 cm^{-1} are shown. In FSD spectra, the region around 1550−1420 cm^{-1} results in a major complexity with bands at 1552 (amide II), 1508 (aromatic skeletal vibration), and 1466 and 1428 cm^{-1} (vibration of graminaceous lignin structures such as vanillyl and syringyl groups). Furthermore, in FSD T spectrum bands at 1737 and 1224 cm^{-1} became apparent, assigned to C−O stretch and O−H deformation of COOH. Absorption at 1224 cm^{-1} is not apparent in FSD C spectrum, whereas an intensity reduction of the peak at 1737 cm^{-1} occurs, indicating the conversion of carboxyl groups into carboxylate groups as a result of iron interaction. Also, changes following Fe^{2+} addition are evident with the reduction of the band at 1428 cm^{-1} and the appearance of a peak at 1113 cm^{-1} in the C spectrum compared to the T one.

Fluorescence Spectra. Contour EEM spectra of the three samples analyzed are shown in **Figure 9**. Sample T (**Figure 9a**) exhibits a peak at $315_{ex}/425_{em}$. After the addition of iron, no modifications in the peak position occur, but a reduction of fluorescence intensity is observed in D and C spectra (**Figure 9b**,**c**).

Conventional fluorescence spectroscopy has been widely applied to the characterization of humic and fulvic acids of various origins and to the study of composted materials obtained from different sources. Peaks located at higher wavelengths (λ_{em} > 500 nm and λ_{ex} > 475−460 nm) have been attributed to aromatic rings bearing at least one electron-donor group and/or to an unsaturated conjugated system capable of a high degree of resonance. Peaks at intermediate wavelengths (λ_{em} > 470−

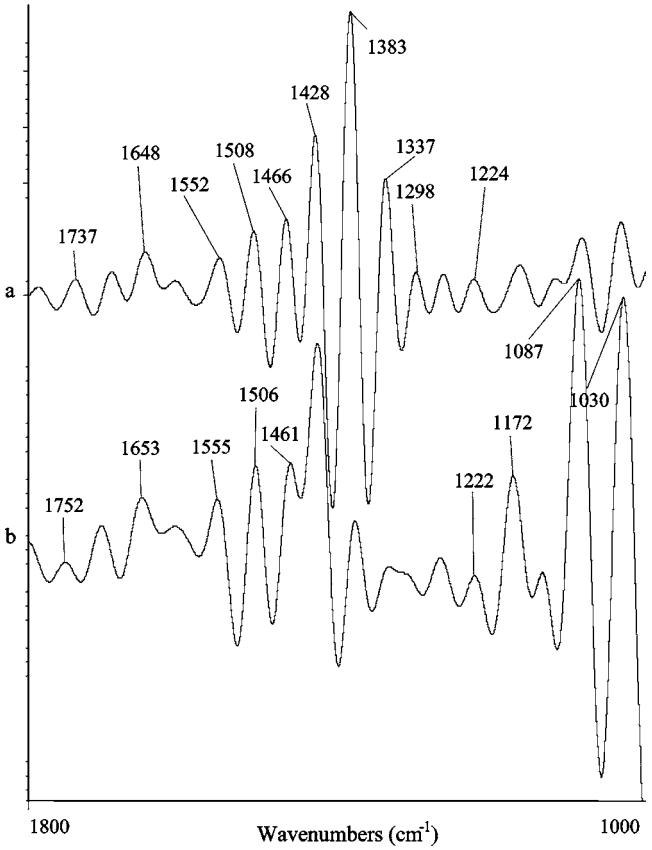

Figure 16. FSD spectra of T sample unheated (**a**) and heated at 350 °C (**b**).

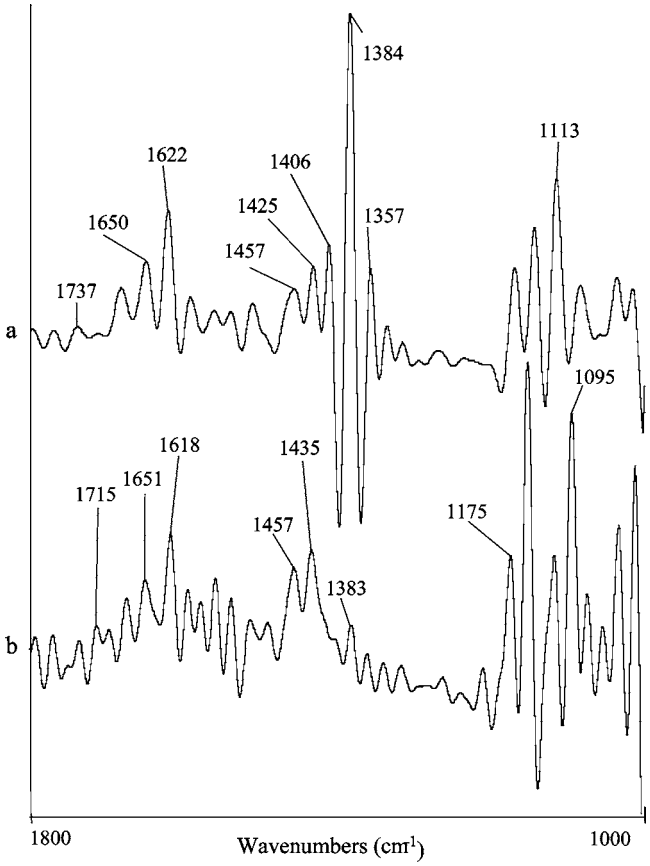

Figure 17. FSD spectra of C sample unheated (**a**) and heated at 350 °C (**b**).

450 nm and λ_{ex} > 390 nm) have been assigned to hydrossicoumarine-like structures originated from lignins and to Shiff base groups −N═C−C═N− obtained by polycondensation of carbonyls with amino groups. Peaks at lower wavelengths (λ_{em} > 540−435 nm and λ_{ex} > 350 nm) have been attributed to phenolic OH conjugated to aromatic ring through a carbonyl group (*22*).

In general, synchronous-scan excitation spectra appear to be more structured and better resolved compared to excitation and emission spectra. They represent the summation of the spectra of several different fluorophores present in the examined molecules, allowing the spectral separation of the fluorescence signals into individual components (*23*, *24*). Synchronous-scan fluorescence spectra of samples analyzed are shown in **Figure 10**. They feature three peaks, respectively, at 350, 388, and 447 nm.

Important changes in fluorescence intensity (FI) of peaks are observed when the three spectra are compared (**Figure 11**). In fact, it is well-known that metal ions, especially paramagnetic ions, are able to quench the fluorescence intensity of organic ligands by enhancing the rate of some nonradiative processes that compete with fluorescence, such as intersystem crossing. Paramagnetic transition ions, such as iron ion, which possess d levels of energy lower than the excited singlet state, may effectively quench the fluorescence of humic ligands via intramolecular energy transfer (*2*).

Following iron addition, FI is reduced for all peaks in D and C spectra, but the peak at 447 nm appears to be more affected by iron interactions, suggesting that the fluorophore responsible for this absorption is mainly involved in iron complexation.

DSC Curves. DSC curves of samples examined are reported in **Figure 12**.

They are similar to previous results obtained on composted materials sampled during composting and in final composts from different sources, including sewage sludges, sawdust, used coffee grounds, farmyard manure, and pulp and paper mill biosludges (*12*−*16*). Thermograms show (a) an endotherm in the low-temperature region (160−180 °C), (b) a very broad exotherm in the medium-temperature region (280 °C), and (c) an exotherm in the high-temperature region (∼500 °C). These thermal effects have been assigned to endotherm under (a) dehydration and/or loss of peripheral polysaccharides chains, exotherm under (b) loss of peptidic structures, and exotherm under (c) oxidation and polycondensation of aromatic nuclei of the molecule. In addition to the above thermal effects, on DSC curves of D and C samples (**Figure 12b**,**c**) further endotherms are apparent, respectively, at 216 and 226 °C (more intense), likely related to Fe^{2+} addition.

To elucidate the functional groups responsible for thermal effects observed by comparison with infrared spectra of unheated samples, FT-IR spectra were carried out on samples heated at 350 and 550 °C (**Figures 13**, **14**, and **15**).

After heating at 350 °C, the total disappearance of peaks at 1384 cm^{-1} is evident for T samples (**Figure 13b**), indicating that the medium-temperature endotherm may be attributed to loss of carboxylate groups. The same results are apparent on spectra of C and D sample heated at 350 °C, but in addition the peak at 1113 cm^{-1} attributed to the vibration of hydrated iron ions is also missing in both C and D spectra (**Figures 14b** and **15b**). This evidence suggests that the endotherm at ∼220 °C is due to carboxylate groups linked with iron ions.

After heating at 550 °C, a few adsorptions are evident on spectra of all samples assigned to lignins (1435 cm^{-1}) (**Figures 13c**, **14c**, and **15c**). Similar results were obtained on pulp and

paper mill biosludges sampled at different composting times (*13*) and were attributed to the high thermostability of lignin structures. Actually, lignins are three-dimensional network polymers of phenylpropane units with many different linkages between the monomers, leading to a complicated and random structure. This explains the stringent conditions necessary for its depolymerization and the inability to bring about reversion to monomers.

In **Figures 16** and **17** are reported FSD spectra in the region of 1800−1000 cm^{-1} of T and C samples unheated (**a**) and heated (**b**) at 350 °C, respectively. FSD spectra of T and C samples heated at 350 °C (**Figures 16b** and **17b**) exhibit a dramatic reduction of the peak at 1384 cm^{-1}, whereas in the FSD spectrum of C sample heated at 350 °C (**Figure 17b**) the disappearance of the peak at 1113 cm^{-1} is very evident. Besides, the appearance of several peaks likely due to combustion products becomes apparent for FSD spectra of both heated samples.

LITERATURE CITED

(1) Marschner, H.; Treeby, M.; Römheld, V. Role of root-induced changes in the rhizosphere for iron acquisition in higher plants. *Z. Pflanzenrhaer. Bodenk.* **1989**, *152*, 197−204.

(2) Senesi, N. Metal-Humic Substances Complexes in the Environment. Molecular and Mechanistic Aspects by Multiple Spectroscopic Approach. In *Biogeochemistry of Trace Metals*; Adriano Domy, C., Ed.; CRC Press: Boca Raton, FL, 1992; Chapter 16, pp 425−491.

(3) Chen, Y.; Barak, P. Iron Nutrition of Plants in Calcareous Soils. *Adv. Agron.* **1982**, *35*, 217−240.

(4) Senesi, N.; Miano, T. M.; Brunetti, G. Humic-like Substances in Organic Amendments and Effects on Native Soil Humic Substances. In *Humic Substances in Terrestrial Ecosystems*; Piccolo, A., Ed.; Elsevier: Amsterdam, The Netherlands, 1996; Chapter 14, pp 531−593.

(5) Jiji, R. D.; Cooper, G. A.; Booksh, K. S. Excitation−Emission Matrix Fluorescence based Determination of Carbamates Pesticides and Polycyclic Aromatic Hydrocarbons. *Anal. Chim. Acta* **1999**, *397*, 61−72.

(6) Provenzano, M. R.; de Oliveira, S. C.; Santiago Silva, M. R.; Senesi, N. Assessment of maturity degree of composts from domestic solid wastes by fluorescence and Fourier transform infrared spectroscopies. *J. Agric. Food Chem.* **2001**, *49*, 5874−5879.

(7) Baker, A. Fluorescence Properties of some Farm Wastes: Implications for Water Quality Monitoring. *Water Res.* **2002**, *36*, 189−195.

(8) Provenzano, M. R.; D'Orazio, V.; Jerzykiewicz, M.; Senesi, N. Fluorescence Behaviour of Metal Complexes of Humic Acids from Different Sources. In *Humic Substances: Nature's Most Versatile Materials*; International Humic Substances Society−20th Anniversary Conference, Boston, July 21−26, 2002; pp 126, 288−290.

(9) Leinweber, P.; Schulten, H. R.; Horte, C. Differential Thermal Analysis, Thermogravimetry and Pyrolisis-Field Ionization Mass Spectrometry of Soil Organic Matter in Particle-Size Fractions and Bulk Soil Samples. *Thermochim. Acta* **1992**, *194*, 175−182.

(10) Giovannini, G.; Lucchesi, S. Differential Thermal Analysis and Infrared Investigations on Soil Hydrophobic Substances. *Soil Sci.* **1984**, *137* (6), 457−463.

(11) Provenzano, M. R.; Senesi, N. Thermal Properties of Standard and Reference Humic Substances by Differential Scanning Calorimetry. *J. Therm. Anal. Calorim.* **1999**, *57*, 517−526.

(12) Provenzano, M. R.; Senesi, N. Differential Scanning Calorimetry of River Aquatic Fulvic Acids and their Metal Complexes. *Fresenius' Environ. Bull.* **1998**, *7*, 423−428.

(13) Provenzano, M. R.; Senesi, N.; Miikki, V. Characterization of Composts and Humic Acids From Pulp and Paper Mill Biosludges by DSC in Association with FT-IR Spectroscopy. *J. Therm. Anal. Calorim.* **1998**, *52*, 1037−1046.

(14) Provenzano, M. R.; Senesi, N.; Piccone, G. Thermal and Spectroscopic Characterization of Organic Matter from Municipal Solid Wastes. *Compost, Sci. Utilization* **1998**, *6* (3), 67−73.

(15) Provenzano, M. R.; Ouatmane, A.; Hafidi M.; Senesi, N. Differential Scanning Calorimetric Analysis of Composted Materials from Different Sources. *J. Therm. Anal. Calorim.* **2000**, *61*, 607−614.

(16) Outmane, A.; Provenzano, M. R.; Hafidi M.; Senesi, N. Compost Maturity Assessment using Calorimetry, Spectroscopy and Chemical Analysis. *Compost Sci. Utilization* **2000**, *8*, 124−143.

(17) Trombetta, A.; Belfiore, G.; Piccone, G. G.; Nappi, P.; Barberis, R. *Metodi di analisi del compost*; Collana Ambiente No. 6, Regione Piemonte, Torino, Italy 1992.

(18) Nicolardot, B.; Germon, J. C.; Chaussod, R.; Catroux, G. Une technique simple pour dèterminer la maturitè des compost urbains. *Compost Information* **1982**, *10*, 2−4.

(19) Stentiford, E. I. Composting control: principles and practice. In *The Science of Composting* de Bertoldi, M., Sequi, P., Lemmes, B., Papi, T., Eds.; Blakie Academic and Professional: London, U.K., 1996; pp 29−39.

(20) Chapman, H. D.; Pratt, P. F. In *Methods of Analysis for Soils, Plants and Wastes*; University of California: Los Angeles, CA, 1961.

(21) Gazzetta Ufficiale Supplemento ordinario *D. M. 11, 5.92: Approvazione dei metodi ufficiali di analisi chimica del suolo;* Serie Generale 121; May 25, 1992.

(22) Senesi, N.; Miano, T. M.; Provenzano, M. R.; Brunetti, G. Characterization, Differentiation, and Classification of Humic Substances by Fluorescence Spectroscopy. *Soil Sci.* **1991**, *152* (4), 259−271.

(23) Miano, T. M.; Senesi, N. Synchronous Excitation Fluorescence Spectroscopy Applied to Soil Humic Substances Chemistry. *Sci. Total Environ.* **1992**, *117/118*, 41−51.

(24) Ahmad, S. R.; Reynolds, D. M. Synchronous Fluorescence Spectroscopy of Wastewater and some Potential Constituents. *Water Res.* **1995**, *29* (6), 1599−1602.

Received for review July 6, 2004. Revised manuscript received November 4, 2004. Accepted November 4, 2004.

JF048889G